减振沟在强夯施工时的减振效果研究

淳 庆[1]，潘建伍[2]
（1. 东南大学 城市与建筑遗产保护教育部重点实验室，南京 210096；2. 南京航空航天大学 土木系，南京 210016）

摘 要： 为研究减振沟在降低强夯振动效应上的影响因素，首先，用 ANSYS/LS－DYNA 有限元软件比较了有无减振沟时的地面峰值加速度分布，分析了不同距离、不同深度、不同宽度减振沟的减振效果。结果表明：减振沟可减小 60%～80% 的振动加速度，减振沟的减振效果随其深度增加而增加，而减振沟的宽度基本不影响减振效果。并通过对理论数据的拟合得出了求解减振沟减振效果的近似公式。然后，结合工程实例进行了现场测试，结果表明：强夯振动持时在 0.2 s 至 0.5 s 之间，峰值加速度一般出现在前 0.1 s 内；径向水平加速度的幅值最大，竖向加速度次之，环向水平加速度相对较小；点夯引起的最大振动通常发生在对同一夯击点的第 6 下夯击时，而满夯引起的最大振动发生在对同一夯击点的第 2 下夯击时；减振沟的减振效果达 50%～90%，与理论分析结果基本一致。

关键词： 强夯；减振沟；振动；数值模拟
中图分类号： TU365 **文献标识码：** A

在第 26 届世界大学生运动会主体育场（位于深圳市龙岗区）的建设过程中发现了清代建造的格坑村老围屋（图 1）。格坑村老围屋为三栋砖混结构，始建于清代，距今已有百年历史，为典型岭南建筑。建筑物底部墙体为砂石夯土墙，上部墙体为砖砌体，砖砌大放脚基础，埋深 0.8m。由于大运城内新建项目的基础较差，填土较厚，业主单位选用了较经济的强夯法对地基进行处理。考虑到格坑村老围屋距离最近的夯击点只有 10m 左右，为减小强夯施工对该历史建筑的破坏程度，业主单位决定在该建筑周围设置减振沟。

强夯施工过程中，当夯锤以冲击力贯入地基时，能量通过夯锤底部和侧面以弹性波传播的应变能形式向外扩散和传递，能量转化为体波和面波传到土里，压缩波首先到达，剪切波次之，瑞利波最后到达。从振波特点来看，主要成分是瑞利波，占到振动能量的 67%，剪切波占 26%，压缩波波占 7%。振源能量的 2/3 由表面波沿地面表层在大约一个波长区域深度内向四周传播引起环境振动，其余 1/3 由体积波向纵深传播起压实作用。随着夯锤入土深度的增加，强夯振动在地面的影响范围也增大[1-4]。减振沟是降低强夯振动效应的有效措施，减振沟主要起到消波、滤波的作用，将大部分振动波的水平分量产生的能量降低到最低限度，同时也使竖向能量有了很大的衰减[1]。为研究影响减振沟减振效果的各种因素，首先通过数值模拟进行了参数分析，为减振沟的设计提供参考；在减振沟施工完成后，通过现场测试考察了减振沟在强夯施工时的实际减振效果。

基金项目：中国博士后科学基金项目（20090450072）；江苏省博士后科学基金项目（0901003c）；东南大学博士后重点科研资助项目
收稿日期：2009－04－07 修改稿收到日期：2009－06－16
第一作者 淳 庆 男，博士后，1979 年 10 月生

图 1 深圳格坑村老围屋
Fig. 1 The round houses of Gekeng Village in Shenzheng

1 减振沟减振效果理论计算

减振沟的深度一般可以按瑞雷波的 1/3 波长或现有的基础埋置深度考虑[1]，强夯时的瑞利波波长通常在 8 m～12 m 之间[5]。为了解强夯施工对老建筑的影响，根据工程地勘报告及相关文献[6-10]，对格坑村老围屋减振几种模型进行了显式动力有限元分析。前处理采用 Ansys 11.0™，求解器采用 Ls－dyna 971R2™，后处理主要采用 Ls－prepost 2.1。Ls－dyna 是一个显式为主的非线性动力分析通用程序，可以求解各种二维和三维非弹性结构的高速碰撞、爆炸和模压等大变形动力响应。

1.1 有限元模型

1.1.1 基本模型

考虑到对称性，只取四分之一模型进行分析，有限元模型的基本尺寸为 30 m 长、30 m 宽、20 m 深。共计算了 6 个模型：（1）不设减振沟；（2）减振沟边缘离夯击点 6 m，深 3 m，宽 1 m；（3）减振沟边缘离夯击点 6 m，深 4 m，宽 1 m；（4）减振沟边缘离夯击点 5 m，深 3 m，宽 1 m；（5）减振沟边缘离夯击点 5 m，深 4 m，宽 1 m；（6）减振沟边缘离夯击点 5 m，深 4 m，宽 2 m。这 6 个模型的有限元模型如图 2 所示。

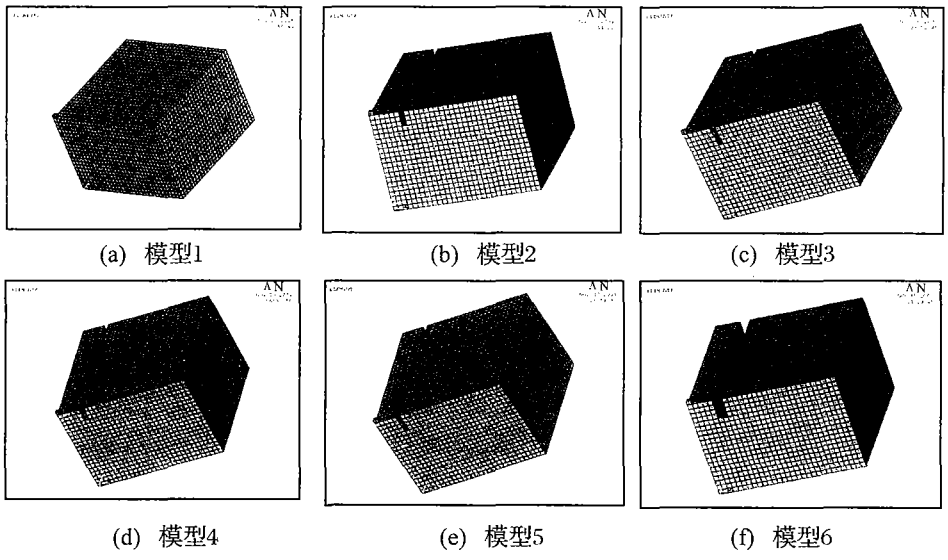

(a) 模型1 (b) 模型2 (c) 模型3

(d) 模型4 (e) 模型5 (f) 模型6

图 2 计算模型

Fig. 2 Computing models

1.1.2 网格划分

采用 Solid164 单元,这是一种 8 节点 6 面体单元,默认采用减缩积分选项。根据有关文献[11],合适的单元长度和波长的关系为:

$$\Delta x \leq \left(\frac{1}{6} \sim \frac{1}{12}\right)\lambda \tag{1}$$

其中,Δx 为单元边长,λ 为所需考虑的波长,由于强夯问题瑞利波影响最大,而强夯引起的瑞利波长一般为 8 m ~ 12 m,因此取单元边长为 1 m 进行网格划分。

1.1.3 材料模型

由于夯锤变形相对较小,简化为刚体。对于土壤的模拟,Ls-dyna 中有第 3、5、147、193 号材料模型可选,本次分析选用 193 号即 Drucker-Prager 弹塑性模型,该模型的主要参数有:密度、剪切模量、泊松比、粘聚力、内摩擦角等。对于地勘报告中没有给出的参数例如地表填土层的材性,参照有关文献[11]的取值。弹性模量按压缩模量放大 5 到 10 倍取值,再换算成剪切模量。

1.1.4 荷载和边界

在两个对称面施加法向位移约束,在除了地表之外的其它表面施加无反射边界。对夯锤施加 15.65 m/s的初速度。由于强夯引起的动力响应峰值通常发生在撞击后的 0.5 s 内,因此计算截止时间取前0.5 s。

1.2 计算结果

从计算结果可以看出,由于填土层较松软,夯击点的变形是很大的。从各时刻的变形看,夯锤撞击地表之后,压实过程在前 0.05 s 内完成,之后根据填土层所取材料参数的不同,开始不同程度的回弹。考察距离夯击点 10 m 处的地表节点的径向即 x 向响应,图 3 ~ 图 8 分别为六种模型前 0.5 s x 向位移、速度和加速度曲线。

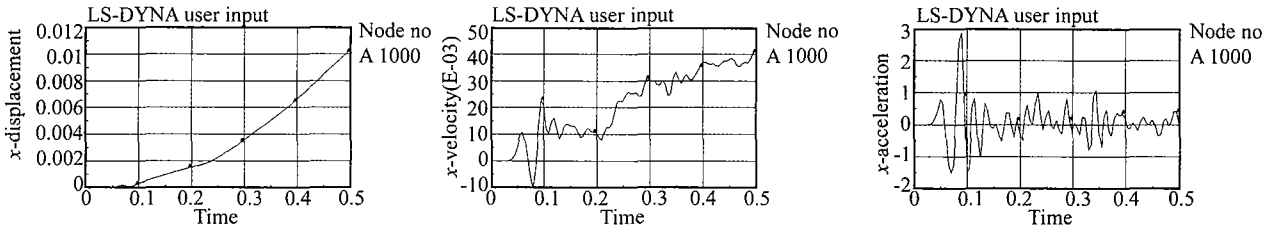

(a) 位移响应 (b) 速度响应 (c) 加速度响应

图 3 模型 1 距离夯击点 10 m 处的节点 x 向响应

Fig. 3 X-direction response of the location 10 m away from the compaction point in model 1

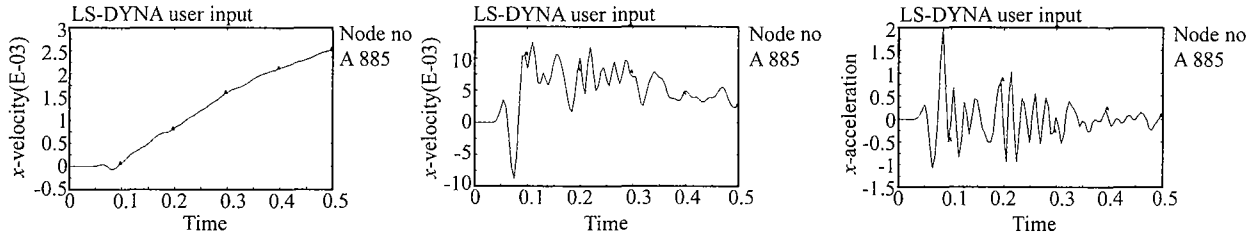

(a) 位移响应 (b) 速度响应 (c) 加速度响应

图 4 模型 2 距离夯击点 10 m 处的节点 x 向响应

Fig. 4 X-direction response of the location 10 m away from the compaction point in model 2

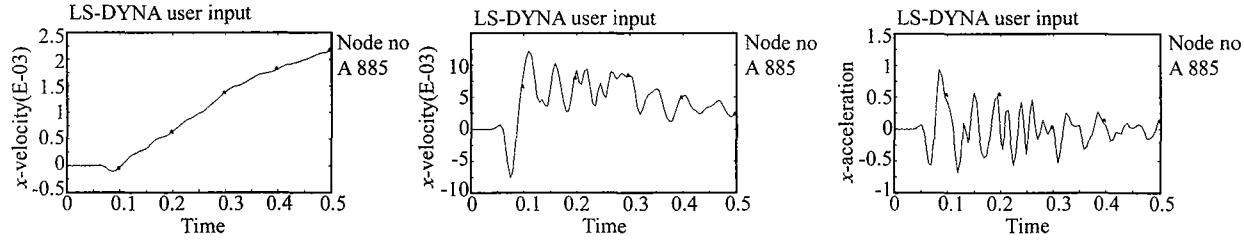

(a) 位移响应　(b) 速度响应　(c) 加速度响应

图 5　模型 3 距离夯击点 10 m 处的节点 x 向响应

Fig. 5 X-direction response of the location 10 m away from the compaction point in model 3

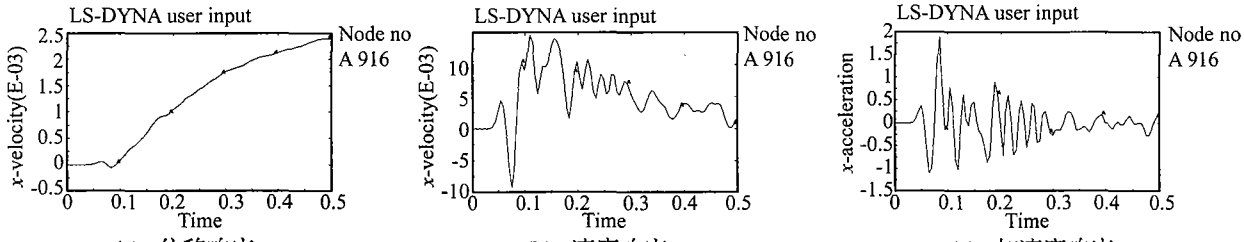

(a) 位移响应　(b) 速度响应　(c) 加速度响应

图 6　模型 4 距离夯击点 10 m 处的节点 x 向响应

Fig. 6 X-direction response of the location 10 m away from the compaction point in model 4

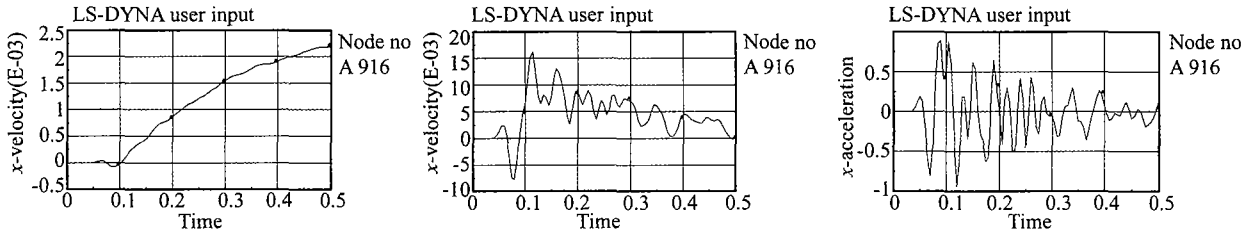

(a) 位移响应　(b) 速度响应　(c) 加速度响应

图 7　模型 5 距离夯击点 10 m 处的节点 x 向响应

Fig. 7 X-direction response of the location 10 m away from the compaction point in model 5

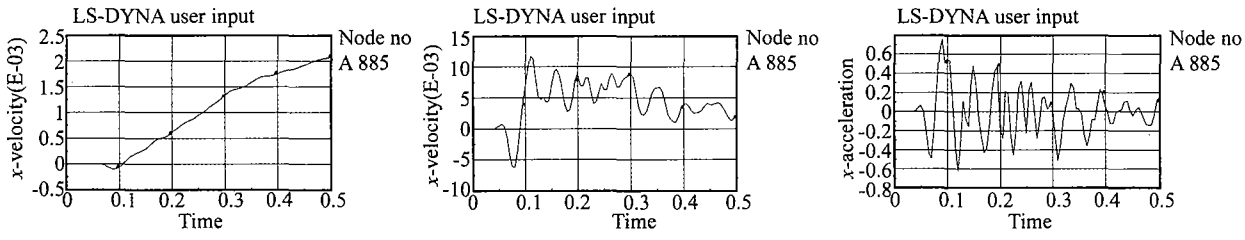

(a) 位移响应　(b) 速度响应　(c) 加速度响应

图 8　模型 6 距离夯击点 10 m 处的节点 x 向响应

Fig. 8 X-direction response of the location 10 m away from the compaction point in model 6

数值模拟结果表明：(1) 减振沟的减振效果可达 60% ~80%；(2) 减振沟的减振效果随其深度增加而增加；(3) 减振沟的宽度基本不影响减振效果，可以不考虑减振沟宽度的影响；(4) 减振沟的减振效果同夯击点与减振沟的距离、拾取点与减振沟的距离以及减振沟的深度近似成线性关系。

本文通过线性回归得出求解水平径向加速度减振程度和竖向加速度减振程度的近似公式，分别见式(1)和式(2)：

$$e_H = 0.065x - 0.024\,8y + 0.095\,1z \quad (1)$$

$$e_V = 0.022\,3x - 0.034\,4y + 0.076\,1z \quad (2)$$

式中：e_H和 e_V分别为水平径向加速度减振程度和竖向加速度减振程度，$\in (0 \sim 1)$；x 为夯击点到减振沟的距离，单位为 m；y 为拾取点到减振沟的距离，单位为 m；z 为减振沟的深度，单位为 m。

2 减振沟减振效果现场检测

为弄清强夯施工时减振沟的实际减振效果以及对该历史建筑的影响程度，在减振沟施工完成后，对最靠近老围屋的两排夯击点的现场强夯施工过程进行了监测。

大运城内新建项目的强夯施工采用二遍点夯和一遍满夯，点夯单击能为 2 500 kN · m，第一遍点夯击数 8 ~ 10击，第二遍点夯击数 6 ~ 8 击；满夯单击能 1 500 kN · m，每点 2 击。强夯重锤 20 t，锤底面积 4 m^2左右。采用强夯处理后的地基承载力特征值将达到 140 kPa，变形模量将达到 15 MPa。

该工程主要地层有：(1) 素填土(①)：灰黄、褐黄、褐红、灰黑等色，由粘性土含少量砂砾组成，层厚 0.3 m ~6.5 m；(2) 粉质粘土 (⑤$_1$)：褐灰，褐黄色，稍为光滑，湿，可塑状，摇振反应无，干强度高，韧性高，层厚 0.3 m ~28.1 m；(3) 细砂(⑤$_2$)：灰白，褐黄色，主要成分为石英质，局部含粘性土 5% 左右，分选性较差，饱和、松散 ~ 稍密，层厚 0.2 m ~ 19.5 m；(4) 淤泥质粘土(⑥$_1$)：黑色，含腐木，具臭味，饱和，软塑状，光滑，摇振反应中等，干强度高，韧性中等，层厚 0.5 m ~ 29.5 m；(5) 粉质粘土(⑥$_2$)：灰白、灰黄色，局部含 20% 左右砂，底部偶夹卵石，湿，可塑 ~ 硬塑. 稍光滑，摇振反应无，干强度高，韧性高，层厚 0.5 m ~ 29 m；(6) 粘土(⑨)：灰黑色、褐色，主要成分为粘土，含少量灰岩质尖棱状角砾及玻璃渣、铁丝等杂物，偶含卵石，饱和，软塑，稍光滑，摇振反应无，干强度中等，韧性中等。

格坑村老围屋的减振沟开挖方案如图 9，现场开挖施工见图 10。

2.1 检测设备

主要设备为：东华测试技术开发有限公司生产的 DH5937 型 8 通道动态信号采集仪(图 11)和 DH202 型加速度传感器。数据处理软件为 DHDAS 数据采集系统，它具有对仪器的参数设置、数据采集和对数据基本的统计分析等功能。

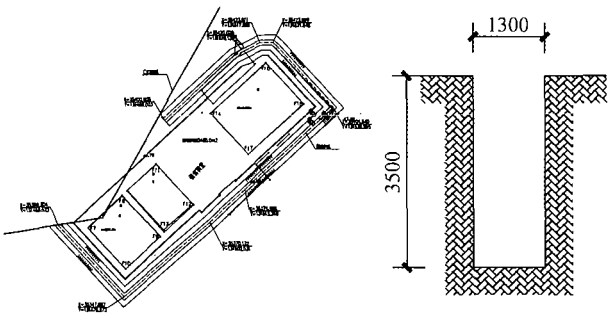

图 9 格坑村老围屋减振沟开挖方案

Fig. 9 Excavation scheme of vibration-isolating slot

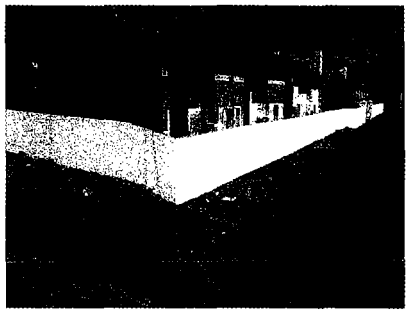

图 10 格坑村老围屋减振沟开挖施工

Fig. 10 Excavation construction of vibration – isolating slot

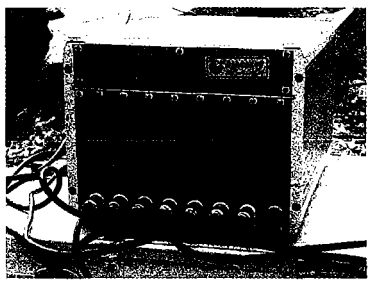

图 11 DH5937 型 8 通道动态信号采集仪

Fig. 11 DH5937-based 8-channels dynamic signal acquisition instrument

2.2 传感器布置

共对 10 个最靠近老围屋的夯击点进行了现场监测，图 12 为这 10 个测点的传感器布置图，图 13 为 4# 夯击点在第 7 次点夯时的传感器加速度记录。

2.3 检测结果

从现场监测数据分析整理，可得出如下主要结果：

减振沟的实际减振效果达 50% ~ 90%，与本文给出的近似公式[式(1)、(2)]计算结果较吻合。

此外，还观测到如下规律：强夯振动持时在 0.2 s 至 0.5 s 之间，峰值加速度一般出现在前 0.1 s 内；径向水平加速度的幅值最大，竖向加速度次之，环向水平加速度相对较小；点夯引起的最大振动通常发生在对同一夯击点的第 6 下夯击时，满夯引起的最大振动发生在对同一夯击点的第 2 下夯击时；点夯引起老围屋底部地表径向水平振动加速度最大值为 0.271 g，竖向振动加速度最大值为 0.180 g，满夯引起老围屋底部地表径向水平振动加速度最大值为 0.237 g。

截至最靠近老围屋的夯击点(距离老围屋约 10 m 至 20 m)的强夯施工完成为止，通过现场观察和检测发现，除局部少量粉饰面层松动掉落外，未发现原有裂缝的扩大、扩展和明显的新裂缝的产生，未发现影响主体结构安全的现象发生。

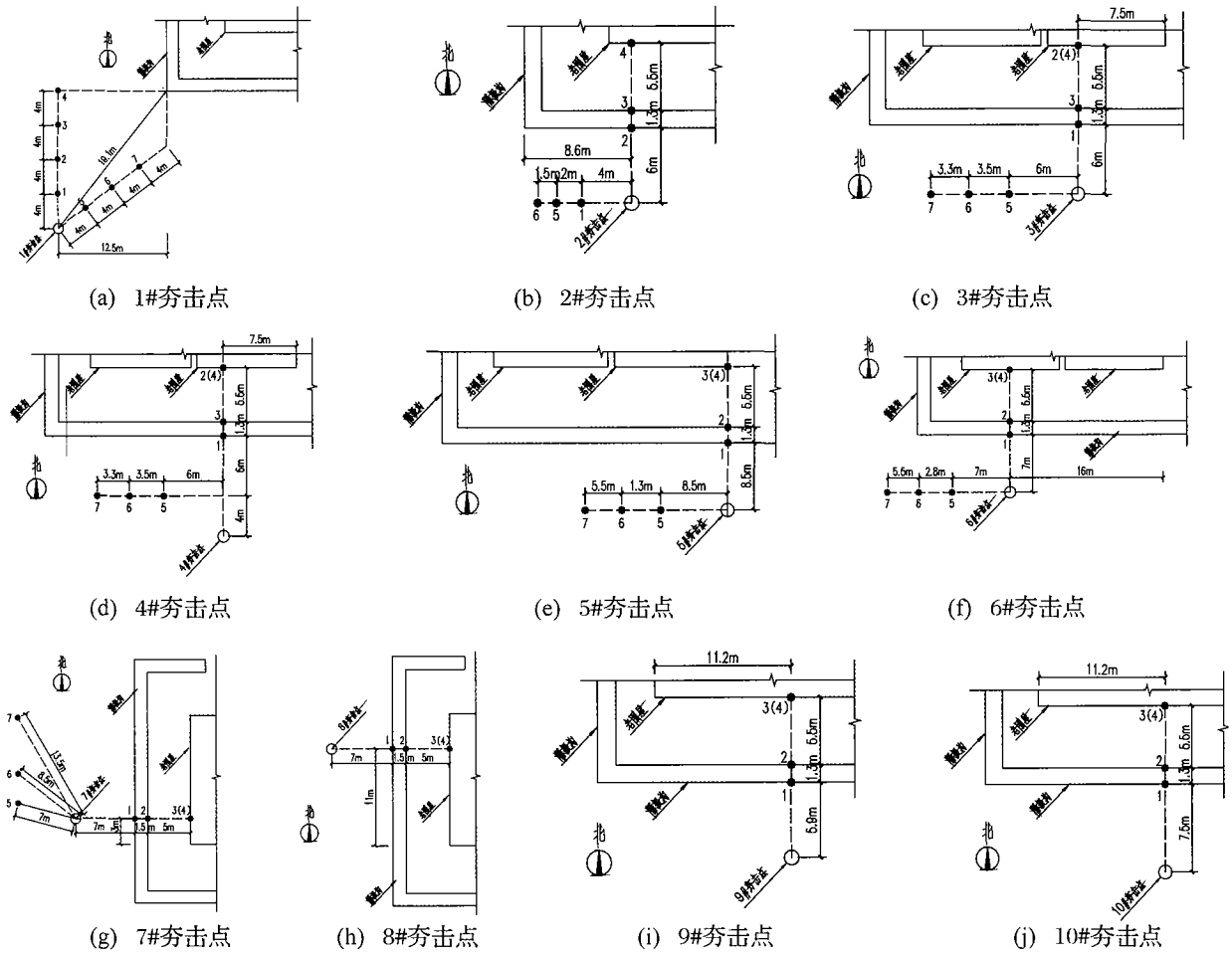

图 12　各测点传感器布置示意图

Fig. 12 Sensors layout

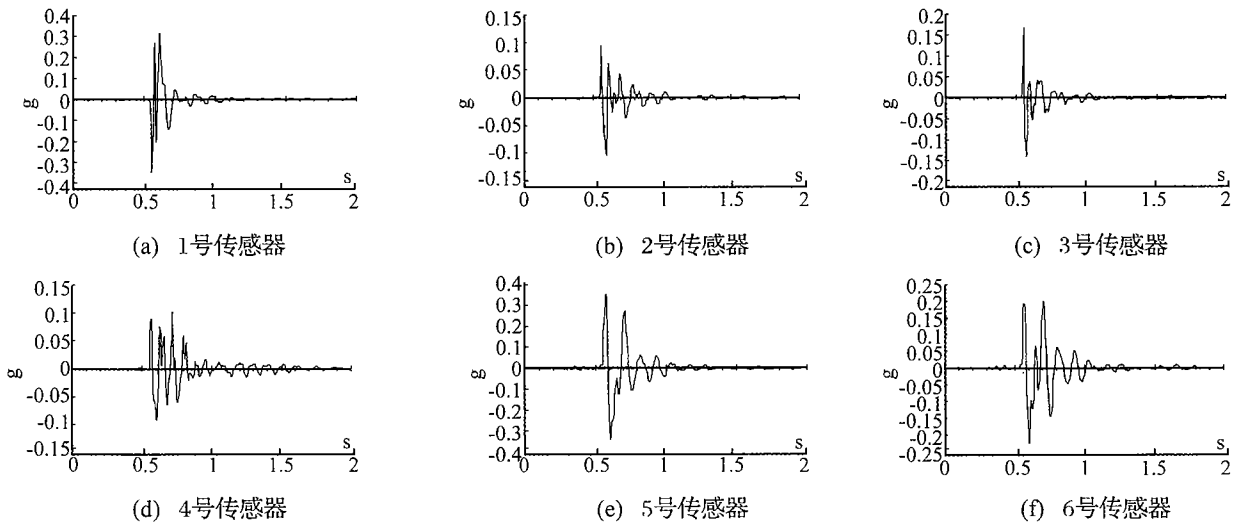

图 13　4#夯击点第 7 次点夯时的加速度记录

Fig. 13 Acceleration record of the 7th compaction at 4# point

3　结　论

本文结合实际工程，通过数值模拟和现场监测对减振沟在强夯施工时的减振效果进行了研究。

现结果比通过数值模拟发现，强夯施工时，减振沟的减振效果显著，减振可达 60% ~80%；减振沟的减振效果随减振沟的深度增加而增加，而减振沟的宽度基本不影响减振效果；减振沟的减振效果同夯击点与减振沟的距离、拾取点与减振沟的距离以及减振沟的深度近似成线性关系。基于此，首次提出了水平径向加

速度减振程度和竖向加速度减振程度的计算公式。

现场监测数据验证了数值模拟结果及减振程度计算公式的正确性,并发现如下规律:强夯振动持时在 0.2 s至0.5 s 之间,峰值加速度一般出现在前 0.1 s 内;强夯引起的径向水平加速度的幅值最大,竖向加速度次之,环向水平加速度相对较小;点夯引起的最大振动通常发生在对同一夯击点的第 6 下夯击时,而满夯引起的最大振动发生在对同一夯击点的第 2 下夯击时。

本文给出的减振程度计算公式可用于类似场地土设置减振沟时的减振效果计算。

参 考 文 献

[1] 沈军明,许 强,等. 小直径异型锤强夯振动对周围建筑物的影响研究[J]. 施工技术, 2006,12(35):11 - 14.

[2] 施有志. 强夯引起的振动规律及环境效应分析[J]. 岩土工程技术,2007,21(3):144 - 148.

[3] 黄 瑛. 强夯对周围已建建筑物的影响[J]. 中国港湾建设,2007,6(3):24 - 26.

[4] 方 磊,经 绯,等. 强夯振动影响与构筑物安全距离研究[J]. 东南大学学报(自然科学版), 2001, 31(3): 29 - 32.

[5] 杨龙才,王炳龙,等. 强夯施工对环境振动的影响分析[J]. 华东交通大学学报,2007,24(2):16 - 20.

[6] 王卫锋,师旭超. 低能强夯工程中隔振沟隔振效果分析[J]. 铜业工程,2007, 2(2):68 - 70.

[7] 梁开水,陈天珠,等. 减震沟减震效果的数值模拟研究[J]. 爆破,2006,23(3):18 - 21.

[8] Pan J L, Selby A R. Simulation of dynamic compaction of loose granular soils[J]. Advances in Engineering Software, 2002,33:631 640.

[9] Lee F H, Gu Q. Method for estimating dynamic compaction effect on sand[J]. Journal of Geotechnical and Geoenvironmental Englneering,2004,130(2):139 - 152.

[10] Hwang J H,Tu T Y. Ground vibration due to dynamic compaction[J]. Soil Dynamics and Earthquake Engineering. 2006,26:337 - 346.

[11] 周向国. 强夯加固回填土的有效加固深度预估与数值模拟[D]. 长沙:长沙理工大学, 2007:45 - 46.

(上接第 87 页)

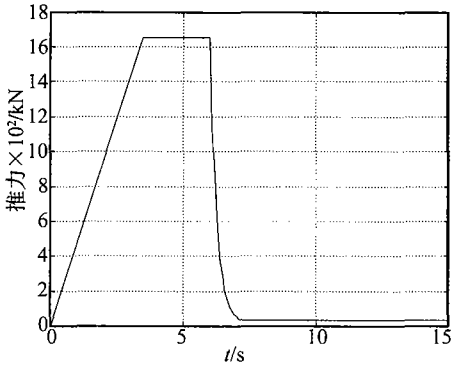

图 7 发动机推力曲线

Fig. 7 Rocket motor thrust

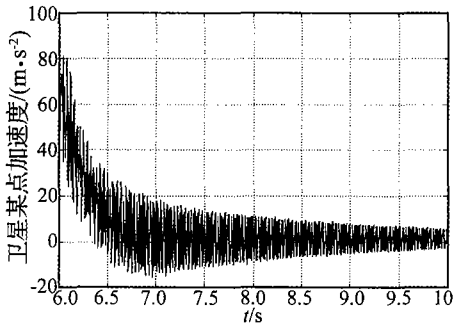

图 8 卫星内部点的加速度响应

Fig. 8 Acceleration response in the satellite

4 结 论

本文介绍的基于传递函数的星箭耦合载荷分析方法经过一个简单算例和一个工程实例验证,表明方法是正确的,并且是可以实现的。

文中给出了工程实例是纵向振动的星箭耦合载荷模型,界面上只有一个纵向位移分量,因此传递函数拟合等运算较为简单。对于星箭耦合载荷的横向振动模型,界面是多自由度的,传递函数拟合方法还有待于进一步研究。

参 考 文 献

[1] 马兴瑞,等. 星箭力学环境分析与试验技术研究进展[J]. 宇航学报,2006,27(3):323 - 331.

[2] 隋允康,等. MSC. Nastran 有限元动力分析与优化设计实用教程[M]. 北京: 科学出版社,2004.

[3] 王文亮,等. 结构振动与动态子结构方法[M]. 上海: 复旦大学出版社,1985.

[4] 赵 阳. 面向整星隔振的星箭耦合载荷分析[D]. 上海: 复旦大学,2004.

[5] Gustavsen B, et. al. Rational approximation of frequency domain responses by vector fitting, IEEE Trans. Power Delivery, 1999,14(3):1052 - 1061.

[6] Karris S T. Introduction to Simulink® with Engineering Applications, Orchard Publications, 2006.

[7] Macia N F, 等著,李乃文等译. 动态系统建模与控制[M]. 北京: 清华大学出版社,2006.

[8] 李 辉,等,基于 MatlabSimulink 的运载火箭 6 自由度运动仿真[J]. 宇航学报,2005,26(5):616 - 619.

[9] 张俊刚,等. 振动试验中力限控制技术[J]. 航天器环境工程,2005,22(5):253 - 256.

[10] Transient Loads from Thrust Excitation (NASA SP-8030), NASA Space Vehicle Design Criteria (Structure).

diate location, and subjected to axial force at the other end were studied. The characteristic equations and the eigenfunctions of the beam were derived in accordance with the corresponding boundary conditions. Using the characteristic equation, the effect of the location of intermediate support on the frequencies was discussed. The differential equation of the beam's motion was discretized by applying Ritz-Galerkin method with the first four eigenfunctions as its trial functions and the instability mechanism corresponding to different location of intermediate support was discussed. It is shown that there exists a special location of intermediate support ξ_1; as the axial pressure p increases from zero, for the location of intermediate support $\xi_b < \xi_f$, the beam becomes unstable due to flutter, and for $\xi_b > \xi_f$, it loses stability due to divergence. At $\xi_b = \xi_f$ the critical force undergoes a jump, implying the transition of instability mode from flutter to divergence.

Key words: beam with intermediate support; frequency; eigenfuntion; stability (pp:101 - 104)

Study on parametrically excited horizontal nonlinear vibration in single-roll driving mill system

ZHANG Rui-cheng, CHEN Zhi-kun, WANG Fu-bin

(College of Computer and Automatic Control, Hebei Polytechnic University, Hebei Tangshan 063009, China)

Abstract: The non-linear equation of horizontal motion of single-roll driving mill was derived based on analyzing the friction between roll and workpiece and considering the nonlinear stiffness and damping of the system. By means of a multiple-scales method, the existence and stability of periodic solutions in a first-order approximation close to the main parametric resonance were investigated, and the frequency-response equation was provided. Bifurcations of the system and regions of chaotic solutions were found. By use of maximal Lyapunov exponent and Poincare map, it shows that vibration of the rolling system appears more complex under larger excitation amplitude.

Key words: rolling mill; nonlinear vibration; parametric excitation; resonance; chaos (pp:105 - 108)

Dynamic analysis of a smart cracked beam based on the reverberation matrix method

YAN Wei, YUAN Li-li

(Faculty of Architectural, Civil Engineering and Environment, Ningbo University, Ningbo 315211, China)

Abstract: A modified model combining electro-mechanical impedance (EMI) technique and reverberation matrix method (RMM) was presented to quantitatively correlate crack parameters with piezoelectric signatures through the proper dynamic analysis of a smart cracked beam. The structural members of the cracked beam were modeled as Timoshenko beams with flexural motion, while the cracks were treated as massless rotational springs. For a structural member with surface-bonded PZT wafers, it can be considered as a coupled structural system. Then, an analytical expression of impedance involving information of cracks was derived. Based on this model, comparison study was implemented between self-conducted experiment and existent research results. Finally, the effects of some physical parameters in regard to crack information on EMI signatures were investigated for structural health monitoring.

Key words: EMI; RMM; crack detection; coupled system (pp:109 - 114)

Vibration-isolating effect of vibration-isolating slot in the process of dynamic compaction construction

CHUN Qing[1], *PAN Jian-wu*[2]

(1. Key Lab of Urban & Architectural Heritage Conservation, Ministry of Education, Southeast University, Nanjing 210096, China;
2. Civil Engineering Department, Nanjing University of Aeronautics and Astronautics, Nanjing 210016, China)

Abstract: ANSYS/LS-DYNA was used to study the influencial factors, on the vibration-isolating effect of vibration-isolating slot under different working conditions. The distributions of peak acceleration in the cases of with and without vibration-isolating slot were compared. The vibration-isolating effects of different distance, different depth and different width of the slot were discussed. The results show that the vibration level can be reduced to 60% ~80%. The vibration-

isolating effect would increase with the increase of depth, but the width of slot has little influence on the vibration-isolating effect. The approximate formulas for evaluating the vibration-isolating effect of vibration-isolating slot were presented by fitting the theoretical data. The field test was then carried out. The results show that the vibration duration caused by dynamic compaction is about 0.2 seconds to 0.5 seconds and the peak acceleration appears within the first 0.1 seconds. The largest acceleration response is the radial horizontal acceleration, followed by the vertical acceleration, and the tangential horizontal acceleration is the least. The largest vibration caused by point compaction often appears at the sixth strike at the compaction point, while the largest response often appears at the second strike at the same point under full compaction. The vibration-isolating effect of vibration-isolating slot reaches 50% ~ 90%, which is consistent with the theoretical results.

Key words: dynamic compaction; vibration-isolating slot; vibration; numerical simulation (pp:115 - 120)

Suction effect on suppressing blade vibration

DING Lei, HE Li-dong, LI Jin-bo

(Diagnosis and Self-Recovery Engineering Research Center, Beijing University of Chemical Technology, Beijing 100029, China)

Abstract: Suction can influence the air performance around blade, and thus can be used to control flow separation along surface of a blade. Variations of blade vibration were studied experimentally with consideration of suction effect. The vibration amplitude of blade was measured at different suction positions or with different gap lengths. The effect of fluid field around blade was analyzed by numerical simulation in different conditions, including at different suction positions and with different suction velocities. However, the impact of gas velocity at tip clearance was emphasized. The laws induced from experimental study and simulation calculation are consistent with each other. Some important conclusions were given in the paper. The vibration could be suppressed due to suction before or above the blade. The maximal attenuation of blade amplitude is up to 27% in the experimental condition.

Key words: suction; blade vibration; vibration suppressing; model experiment; numerical simulation; gas velocity at tip clearance (pp:121 - 124)

Approximate entropy analysis for structural damage detection under moving load

WANG Bu-yu, YU Ya-nan

(College of Civil Engineering and Architecture, Zhejiang University, Hangzhou 310058, China)

Abstract: The nonlinear character and magnitude of structural vibration will vary with the distance between load point and damage position, based on that the structural damage information can be extracted. Putting a moving load on the structure, and calculating the approximate entropy value of vibration data, the nonlinear eigenvalue was then extracted as the feature for structural damage pattern recognition by using neural network. The validity of the method was reviewed by an example of beam under moving load, which reinforces the structural nonlinear character. The results of simulation and experiment show that approximate entropy can figure the nonlinear grade of signal availably, and it is not sensitive to noise. So, it can be taken as the eigenvectors in pattern recognition based on neural network.

Key words: structure; moving load; approximate entropy; damage detection; neural network (pp:125 - 128)

Nonlinear finite element analysis for galloping of iced bundled conductors

LIU Xiao-hui[1], *YAN Bo*[1], *ZHANG Hong-yan*[2], *ZHOU Song*[3], *TANG Jie*[3]

(1. Department of Engineering Mechanics, Chongqing University, Chongqing 400044, China;
2. Sichuan Electric Power Test & Research Institute, Chengdu 610071, China;
3. Sichuan Electric Power Industry Commission & Test Institute, Chengdu 610016, China)

Abstract: A nonlinear finite element analysis for iced bundled conductor, considering the geometric nonlinearity of